Journal of Computational and Applied Mathematics 236 (2012) 3160–3173

Contents lists available at SciVerse ScienceDirect

Journal of Computational and Applied Mathematics

journal homepage: www.elsevier.com/locate/cam

Numerical simulation and linear well-posedness analysis for a class of three-phase boundary motion problems

Zhenguo Pan [a,*], Brian Wetton [b]

[a] Department of Mathematics, National University of Singapore, Singapore 119076, Singapore

[b] Department of Mathematics, University of British Columbia, Vancouver, B.C. Canada V6T 1Z2

ARTICLE INFO

Article history:
Received 16 February 2011
Received in revised form 25 January 2012

Keywords:
Grain boundary
Curvature motion
Surface diffusion
Three-phase problem
Well-posedness

ABSTRACT

We investigate the linear well-posedness for a class of three-phase boundary motion problems and perform some numerical simulations. In a typical model, three-phase boundaries evolve under certain evolution laws with specified normal velocities. The boundaries meet at a triple junction with appropriate conditions applied. A system of partial differential equations and algebraic equations (PDAE) is proposed to describe the problems. With reasonable assumptions, all problems are shown to be well-posed if all three boundaries evolve under the same evolution law. For problems involving two or more evolution laws, we show the well-posedness case by case for some examples. Numerical simulations are performed for some examples.

1. Introduction

We consider a class of three-phase boundary motion problems in two dimensions as shown in Fig. 1. There are three phases in this model, denoted by I, II and III respectively. Their interfaces Γ_1, Γ_2 and Γ_3 evolve with parabolic normal velocities given by curvature or its even order derivatives with respect to arc length. They meet at a triple junction with prescribed angles θ_1, θ_2 and θ_3. Extra junction conditions may be necessary depending on the motion of the interfaces.

We first consider the simplest case for which the normal velocity of the interface Γ_i is proportional to its curvature. This is the well known curvature motion which models the evolution of grain boundaries in materials science. In this model, the normal velocity of Γ_i is given by

$$V_i = A_i \kappa_i \tag{1}$$

where V_i represents the normal velocity of Γ_i and κ_i is curvature. The coefficient $A_i = a_i \gamma_i$ is a physical constant where a_i and γ_i are the mobility and the surface energy of the grain boundary Γ_i respectively. This motion has been studied in, for example, [1–7]. A comprehensive introduction with physical background is available in [8].

The phase boundaries in this model can be described by parametrized curves $X_i(\sigma, t)$ with parameter $\sigma \in [0, \infty)$ with $\sigma = 0$ corresponding to the junction. Here, X denotes a quantity with two components (x, y) in 2D. With this formulation, curves that are not single valued functions can be described. An additional numerical advantage of this parametrized curve formulation is that the junction is a fixed boundary condition, not a free boundary one. For general parametrized curves in

* Corresponding author.
E-mail addresses: panzhenguo@gmail.com (Z. Pan), wetton@math.ubc.ca (B. Wetton).

0377-0427/$ – see front matter © 2012 Elsevier B.V. All rights reserved.
doi:10.1016/j.cam.2012.02.013

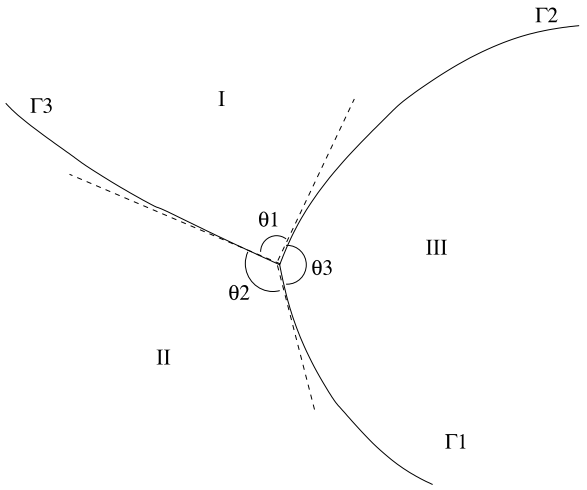

Fig. 1. A three-phase geometry.

2D, the tangent T and normal N vectors and the curvature κ can be described as follows

$$\begin{aligned} T &= \frac{\partial_\sigma X}{|\partial_\sigma X|}, \\ N &= T^\perp, \\ \kappa &= \frac{\partial_\sigma^2 X \cdot N}{|\partial_\sigma X|^2}. \end{aligned} \tag{2}$$

The expected normal motion is achieved when the following equation is satisfied,

$$\partial_t X_i \cdot N_i = \kappa_i \tag{3}$$

for $i = 1, 2, 3$, where κ_i and N_i can be replaced by the expressions in Eq. (2). Notice that the tangential velocity away from the junction can be chosen arbitrarily which leads to different parametrization for the curves. An additional condition to specify the parametrization with good numerical properties was proposed in [7] and independently in [9], which is given as

$$\partial_\sigma X_i \cdot \partial_\sigma^2 X_i = 0. \tag{4}$$

This enforces that the parametrization remains a scaled arc length, although the scaling can change in time for finite length curves. This is seen by rewriting the condition above as

$$\frac{1}{2}\partial_\sigma |\partial_\sigma X_i|^2 = 0.$$

The grain boundary motion with three phases can then be described by

$$\begin{aligned} &\partial_t X_i \cdot N_i = A_i \kappa_i, \quad i = 1, 2, 3, \\ &\partial_\sigma X_i \cdot \partial_\sigma^2 X_i = 0, \quad i = 1, 2, 3 \end{aligned} \tag{5}$$

where constant $A_i = a_i \gamma_i$ depends on the type of the material. This system involves both time dependent partial differential equations (PDE) and elliptic equations. When discretized, the elliptic equations become algebraic equations (AE) and therefore, it is referred to as a PDAE formulation. More details about the idea of using algebraic equations to impose uniform grid spacing are discussed in [7].

The junction conditions for the parametrized formulation above are

$$\begin{aligned} &X_1(0, t) = X_2(0, t) = X_3(0, t), \\ &\frac{\partial_\sigma X_1(0, t)}{|\partial_\sigma X_1(0, t)|} \cdot \frac{\partial_\sigma X_2(0, t)}{|\partial_\sigma X_2(0, t)|} = \cos\theta_3, \\ &\frac{\partial_\sigma X_1(0, t)}{|\partial_\sigma X_1(0, t)|} \cdot \frac{\partial_\sigma X_3(0, t)}{|\partial_\sigma X_3(0, t)|} = \cos\theta_2 \end{aligned} \tag{6}$$

where the first identity guarantees that the triple junction does not pull apart and the two angle conditions come from Young's law indicating the balance of surface tensions. The values of θ_i are given. For the convenience of discussion, we will

also use the arc parameter s in addition to the scaled arc length parameter σ. For example, the junction conditions above can be simply expressed as

$$\begin{aligned} &X_1(0,t) = X_2(0,t) = X_3(0,t),\\ &\partial_s X_1(0,t)\cdot\partial_s X_2(0,t) = \cos\theta_3,\\ &\partial_s X_1(0,t)\cdot\partial_s X_3(0,t) = \cos\theta_2. \end{aligned} \tag{7}$$

We remark that the value of angle θ_i depends on the surface energy γ_i and the two angle conditions are equivalent to:

$$\gamma_1\partial_s X_1 + \gamma_2\partial_s X_2 + \gamma_3\partial_s X_3 = 0. \tag{8}$$

There are other formulations that can describe this grain boundary motion problem, for example, the parabolic formulation discussed in [1,2]. A linearization of the system shows that it is parabolic in both components and therefore it is convenient for theoretic analysis. In [1], the short time existence and uniqueness of the problem with $A_i = 1$ were investigated based on the parabolic formulation. One may also use a Cartesian formulation when all interfaces can be represented by single-valued functions. However, the extension of these formulations to higher order problems is difficult, or even impossible.

A more complicated three-phase boundary motion problem is discussed in [10,11]. Instead of the second order curvature motion, the three curves evolve by surface diffusion with normal velocity being proportional to the surface Laplacian of mean curvature. In two dimensions, the normal velocity is reduced to the negative second derivative of curvature with respect to arc length, i.e.

$$V_i = -B_i\partial_s^2\kappa_i, \tag{9}$$

where $B_i = b_i\gamma_i$ is a physical constant with a similar meaning as A_i.

Applying the same idea as for the curvature motion, one has the following PDAE formulation for the motion by surface diffusion:

$$\begin{aligned} &\partial_t X_i\cdot N_i = -B_i\partial_s^2\kappa_i, \quad i = 1,2,3,\\ &\partial_\sigma X_i\cdot\partial_\sigma^2 X_i = 0, \quad i = 1,2,3. \end{aligned} \tag{10}$$

Here we point out that the system is always given in terms of σ. However, we frequently use the arc length parameter s to simplify the expressions. For example, when the normal velocity $\partial_s^2\kappa$ is denoted in terms of σ, it becomes

$$\partial_s^2\kappa = \frac{\partial_\sigma^2\kappa}{|\partial_\sigma X|^2},$$

noticing the property that σ is scaled arc length.

This system requires nine junction conditions at $\sigma = 0$ which are given as follows:

$$\begin{aligned} &X_1(0,t) = X_2(0,t) = X_3(0,t),\\ &\partial_s X_1(0,t)\cdot\partial_s X_2(0,t) = \cos\theta_3,\\ &\partial_s X_1(0,t)\cdot\partial_s X_3(0,t) = \cos\theta_2,\\ &b_1\gamma_1\kappa_1 + b_2\gamma_2\kappa_2 + b_3\gamma_3\kappa_3 = 0,\\ &\gamma_1\partial_s\kappa_1 = \gamma_2\partial_s\kappa_2 = \gamma_3\partial_s\kappa_3, \end{aligned} \tag{11}$$

where the fourth equation comes from the continuity of chemical potentials and the last equation represents the balance of mass flux.

A parabolic formulation also exists for this problem as discussed in [11,12]. Using a similar technique as in [1], the authors proved the well-posedness of the fourth order system in [11].

Another model is a mixed order problem which is called coupled surface and grain boundary motion. In this model, one of the interface follows curvature motion and the other two interfaces follow motion by surface diffusion. This models some physical details of grain growth in the annealing process when the grain boundary is attached to a free surface. It was first considered by Mullins in [13] where he analyzed the mechanism and formulated the equation to describe the problem. As an important phenomenon controlling the grain growth in material processing and synthesis, the coupled surface and grain boundary motion has been widely studied both experimentally and numerically [9,14–19,13,20,7,21–23].

A PDAE formulation is proposed in [7] for this coupled problem. We assume Γ_1 is the grain boundary and Γ_2, Γ_3 are the two free surfaces. In the literature, it is also assumed that phase II and phase III are of the same material and therefore $\gamma_2 = \gamma_3$. The formulation is then given by

$$\begin{aligned} &\partial_t X_1\cdot N_1 = A\kappa_1,\\ &\partial_t X_i\cdot N_i = -B\partial_s^2\kappa_i, \quad i = 2,3,\\ &\partial_\sigma X_i\cdot\partial_\sigma^2 X_i = 0, \quad i = 1,2,3. \end{aligned} \tag{12}$$

The eight junction conditions are

$$\begin{aligned} &X_1(0,t) = X_2(0,t) = X_3(0,t),\\ &\partial_s X_1(0,t)\cdot\partial_s X_2(0,t) = \cos\theta_3,\\ &\partial_s X_1(0,t)\cdot\partial_s X_3(0,t) = \cos\theta_2,\\ &\kappa_2 + \kappa_3 = 0,\\ &\partial_s\kappa_2 = \partial_s\kappa_3. \end{aligned} \tag{13}$$

The well-posedness for this mixed order problem was discussed in [7]. Due to the presence of mixed order equations, the approach used in [1,11] for equal order problems is not applicable. Instead, the analysis for the mixed order system is implemented by linearizing around fixed straight line solutions which gives a system that has the same highest order behavior as the original problem near the triple junction. The linear system is then investigated and gives an indication about the original problem. This is also the approach that will be used in the current paper.

A parabolic formulation is also available for this coupled problem. A detailed discussion can be found in [12].

The goal of this paper is to generalize the three problems discussed above to a class of three-phase boundary motion problems. We propose a general formulation to describe the problems in this class. The well-posedness of these problems are investigated in a reduced, linear setting with some simplifications. All problems in our class are shown to be well-posed if all three boundaries evolve under the same evolution law. For problems involving two or more types of motion we show the well-posedness case by case for some examples. Numerical simulations for some higher order problems in this class are also performed.

Many approaches have been developed to simulate the evolution of these three-phase problems, e.g., front-tracking methods, level set methods, threshold dynamics algorithms and phase field methods.

The front-tracking methods (e.g., [2,7,24]) use a set of particles to describe the interface and the location of the interface is determined by tracking the motion of these particles. This approach is efficient and usually easy to apply since it explicitly approximates the motion of the interfaces. The computational cost is relatively low as it is implemented over a lower dimensional space compared to other methods. However, it is usually impossible, or difficult, to track topological changes. The authors in [2] managed to track the topological changes for curve networks moving with curvature motion and reasonable results were achieved. In that case, all possible topological changes were discussed and handled separately which is usually not possible for more complicated problems. The numerical method discussed in this paper is basically a front-tracking method as the location of the phase boundaries is tracked explicitly.

The level set methods developed in [25,26] can naturally capture the topological changes of the interface which is embedded as the zero level set of a signed distance function. Attempts to extend the level set methods to three-phase or multi-phase problems have been studied in, for example, [4,27,28]. For multi-phase problems, each phase is represented by a separate level set function and therefore level set methods suffer from establishing appropriate constraints to couple all functions at the junction, especially for mixed order problems.

The threshold dynamics algorithms, also called MBO algorithms, is introduced in [29,4], and studied later in [30–32]. It uses a 1(inside)–0(outside) characteristic function to describe regions separated by the interface. The characteristic function is evolved by diffusion and the resulting function is thresholded to locate the new position of the interface. These methods experience the same difficulty for multiple-phase problems as the level set methods do.

The phase field methods model a phase boundary by a diffusive interfacial layer. To be more precise, the multi-phase structure is described by continuous functions which have nearly constant values in each phase and vary gradually in a narrow region around the phase boundaries. The governing equations are derived based on thermodynamic and kinetic principles which contain a parameter representing the width of the interfacial layer. The position of the interfaces is implicitly given by the zero level set of the evolutionary functions. A similar discussion can also be applied to the mixed order problem as studied in [33–35]. Numerical simulations were also discussed based on these phase field models for both the equal order problems [36,37] and the mixed order problem [38] using either finite difference discretization or finite element methods. The disadvantage of this approach is that the construction of the system depends on the motion type of the phase boundaries.

The paper is organized as follows. In Sections 2 and 3, we propose a general formulation to describe the problems and investigate the linear well-posedness for all equal order problems and some mixed order problems, respectively. In Section 4, we demonstrate numerical simulations for some examples. A conclusion is given in Section 5.

2. Equal order problems

In this section, we consider equal order problems when all three phase boundaries evolve under the same evolution law.

2.1. Mathematical formulation

We generalize the problems discussed in Section 1 as the following three-phase boundary motion problem:

$$\begin{aligned} &\partial_t X_i\cdot N_i = (-1)^{m_i} A_i \partial_s^{2m_i}\kappa_i, \quad i = 1,2,3,\\ &\partial_\sigma X_i\cdot\partial_\sigma^2 X_i = 0, \quad i = 1,2,3, \end{aligned} \tag{14}$$

where A_i are constants coefficients and m_i are non-negative integers satisfying,

$$0 \le m_1 \le m_2 \le m_3. \tag{15}$$

In this section, we consider the equal order case, that is when $m_1 = m_2 = m_3 = m$. The mixed order case will be discussed in the following section.

To propose appropriate junction conditions for these higher order problems, we first assume all phases are of the same material and therefore $A_1 = A_2 = A_3$. For convenience, we take $A_i = 1$ since appropriate spatial scaling can make them unity. Later in this section, we shall also consider examples that A_i are not the same.

We summarize and follow the pattern in the junction conditions for the lower order problems introduced before to propose the following junction conditions:

$$\begin{aligned}
&X_1(0,t) = X_2(0,t) = X_3(0,t),\\
&\partial_s X_1(0,t)\cdot\partial_s X_2(0,t) = \cos\theta_3,\\
&\partial_s X_1(0,t)\cdot\partial_s X_3(0,t) = \cos\theta_2,\\
&\partial_s^{2i-2}\kappa_1 + \partial_s^{2i-2}\kappa_2 + \partial_s^{2i-2}\kappa_3 = 0, \quad i = 1,\dots,m,\\
&\partial_s^{2i-1}\kappa_1 = \partial_s^{2i-1}\kappa_2 = \partial_s^{2i-1}\kappa_3, \quad i = 1,\dots,m,
\end{aligned} \tag{16}$$

where $\theta_2 = \theta_3 = 2\pi/3$ since we assume $A_1 = A_2 = A_3 = 1$. We first notice that each equal order problem requires $3m+6$ junction conditions. We then construct conditions using the derivatives of curvature from order 0 to order $2m-1$. Among the two conditions with the highest derivatives,

$$\partial_s^{2m-1}\kappa_1 = \partial_s^{2m-1}\kappa_2 = \partial_s^{2m-1}\kappa_3 \tag{17}$$

reflects the balance of mass flux noticing that the normal velocity is given by $V = (-1)^m\partial_s^{2m}\kappa$ and

$$\partial_s^{2m-2}\kappa_1 + \partial_s^{2m-2}\kappa_2 + \partial_s^{2m-2}\kappa_3 = 0 \tag{18}$$

reflects the continuity of a sort of potential that produces the mass flow along the interface.

For $m = 0, 1$ these junction conditions match those physical conditions in (25) for the curvature motion and those in (11) for the surface diffusion motion.

2.2. Linear well-posedness

We use the approach discussed in [7] to show the well-posedness of the generalized equal order problems described above.

The basic approach is to linearize the problems around fixed straight line solutions at the junction and investigate the resulting linear system.

We consider linearizing curve $X_i(\sigma, t)$ around the tangential direction at the triple junction. One has

$$X_i(\sigma,t) = d_i\sigma + \epsilon\bar{X}_i(\sigma,t) + O(\epsilon^2), \quad i = 1,2,3,$$

where d_i is a constant vector that represents the unit tangential direction for curve X_i at the triple junction. The term $\epsilon\bar{X}_i(\sigma, t)$ represents a small perturbation to the tangential direction. Substituting the expressions above into system (14) and keeping only the leading order terms ($O(\epsilon)$) yield a linear system about $\bar{X}_i$:

$$\begin{aligned}
&\partial_t\bar{X}_i\cdot d_i^{\perp} = (-1)^m\partial_\sigma^{2m+2}\bar{X}_i\cdot d_i^{\perp}, \quad i = 1,2,3,\\
&d_i\cdot\partial_\sigma^2\bar{X}_i = 0, \quad i = 1,2,3.
\end{aligned} \tag{19}$$

The junction conditions can be linearized analogously to obtain

$$\begin{aligned}
&\bar{X}_1(0,t) = \bar{X}_2(0,t) = \bar{X}_3(0,t),\\
&d_1\cdot\partial_\sigma\bar{X}_2 + d_2\cdot\partial_\sigma\bar{X}_1 - (d_1\cdot d_2)(d_1\cdot\partial_\sigma\bar{X}_1 + d_2\cdot\partial_\sigma\bar{X}_2) = 0,\\
&d_1\cdot\partial_\sigma\bar{X}_3 + d_3\cdot\partial_\sigma\bar{X}_1 - (d_1\cdot d_3)(d_1\cdot\partial_\sigma\bar{X}_1 + d_3\cdot\partial_\sigma\bar{X}_3) = 0,\\
&\partial_\sigma^{2i}\bar{X}_1\cdot d_1^{\perp} + \partial_\sigma^{2i}\bar{X}_2\cdot d_2^{\perp} + \partial_\sigma^{2i}\bar{X}_3\cdot d_3^{\perp} = 0, \quad i = 1,\dots,m,\\
&\partial_\sigma^{2i+1}\bar{X}_1\cdot d_1^{\perp} = \partial_\sigma^{2i+1}\bar{X}_2\cdot d_2^{\perp} = \partial_\sigma^{2i+1}\bar{X}_3\cdot d_3^{\perp}, \quad i = 1,\dots,m.
\end{aligned} \tag{20}$$

Without loss of generality, we specify one of the tangential directions, for example, $d_1 = (0,-1)^T$. With the equal angle condition, one has

$$d_1 = \begin{pmatrix} 0\\ -1\end{pmatrix}, \qquad d_2 = \begin{pmatrix} -\frac{\sqrt{3}}{2}\\ \frac{1}{2}\end{pmatrix}, \qquad d_3 = \begin{pmatrix} \frac{\sqrt{3}}{2}\\ \frac{1}{2}\end{pmatrix}.$$

We shall solve the linearized system (19) exactly using the Laplace transform. We start with the second equation in (19) which is a fixed second order to derive a relation between the two components of $\bar{X}_i$ and substitute it back to the first equation and then solve by the Laplace transform. Let $\tilde{X}_i = (\tilde{u}_i, \tilde{v}_i)$ represent the Laplace transform of $\bar{X}_i = (\bar{u}_i, \bar{v}_i)$ and the transformed system has solutions in the form

$$\begin{aligned}
\tilde{u}_1 &= \sum_{j=1}^{m+1} C_{1j} e^{\lambda_j \sigma}, \\
\tilde{v}_1 &= C_{1,m+2}, \\
\tilde{u}_i &= \sum_{j=1}^{m+1} C_{ij} e^{\lambda_j \sigma} + C_{i,m+2}, \quad i = 2, 3, \\
\tilde{v}_i &= -k_i \left(\sum_{j=1}^{m+1} C_{ij} e^{\lambda_j \sigma} \right) + \frac{1}{k_i} C_{i,m+2}, \quad i = 2, 3,
\end{aligned} \tag{21}$$

where k_i represents the ratio of the two components of d_i. The notation λ_j are roots of equation $\lambda^{2m+2} = (-1)^m s$ satisfying

$$\frac{\pi}{2} < \arg(\lambda_j) < \frac{3\pi}{2}. \tag{22}$$

Here s stands for the Laplace transform variable. We consider values of s in the right half plane:

$$|\arg(s)| < \frac{\pi}{2}. \tag{23}$$

Thus both s and the roots of s have positive real part.

To show the well-posedness for the original problem we only need to prove that there is a unique solution for the coefficients C_{ij} introduced in (21). Substitute the solutions (21) into the linearized boundary conditions (20) to obtain a linear system about C_{ij} with the coefficient matrix M of size $3m + 6$ which is given as below:

$$\begin{pmatrix}
1 & \cdots & 1 & 0 & -1 & \cdots & -1 & -1 & 0 & \cdots & 0 & 0 \\
0 & \cdots & 0 & 1 & -\sqrt{3} & \cdots & -\sqrt{3} & \frac{\sqrt{3}}{3} & 0 & \cdots & 0 & 0 \\
1 & \cdots & 1 & 0 & 0 & \cdots & 0 & 0 & -1 & \cdots & -1 & -1 \\
0 & \cdots & 0 & 1 & 0 & \cdots & 0 & 0 & \sqrt{3} & \cdots & \sqrt{3} & -\frac{\sqrt{3}}{3} \\
\lambda_1 & \cdots & \lambda_{m+1} & 0 & 2\lambda_1 & \cdots & 2\lambda_{m+1} & 0 & 0 & \cdots & 0 & 0 \\
\lambda_1 & \cdots & \lambda_{m+1} & 0 & 0 & \cdots & 0 & 0 & 2\lambda_1 & \cdots & 2\lambda_{m+1} & 0 \\
\lambda_1^2 & \cdots & \lambda_{m+1}^2 & 0 & -2\lambda_1^2 & \cdots & -2\lambda_{m+1}^2 & 0 & -2\lambda_1^2 & \cdots & -2\lambda_{m+1}^2 & 0 \\
\lambda_1^3 & \cdots & \lambda_{m+1}^3 & 0 & 2\lambda_1^3 & \cdots & 2\lambda_{m+1}^3 & 0 & 0 & \cdots & 0 & 0 \\
\lambda_1^3 & \cdots & \lambda_{m+1}^3 & 0 & 0 & \cdots & 0 & 0 & 2\lambda_1^3 & \cdots & 2\lambda_{m+1}^3 & 0 \\
\vdots & \vdots & \vdots & \vdots & \vdots & \vdots & \vdots & \vdots & \vdots & \vdots & \vdots & \\
\lambda_1^{2m} & \cdots & \lambda_{m+1}^{2m} & 0 & -2\lambda_1^{2m} & \cdots & -2\lambda_{m+1}^{2m} & 0 & -2\lambda_1^{2m} & \cdots & -2\lambda_{m+1}^{2m} & 0 \\
\lambda_1^{2m+1} & \cdots & \lambda_{m+1}^{2m+1} & 0 & 2\lambda_1^{2m+1} & \cdots & 2\lambda_{m+1}^{2m+1} & 0 & 0 & \cdots & 0 & 0 \\
\lambda_1^{2m+1} & \cdots & \lambda_{m+1}^{2m+1} & 0 & 0 & \cdots & 0 & 0 & 2\lambda_1^{2m+1} & \cdots & 2\lambda_{m+1}^{2m+1} & 0
\end{pmatrix}.$$

Note that the fifth and sixth row have been multiplied through by $-2\sqrt{3}/3$ and $2\sqrt{3}/3$, respectively.

Appropriate manipulation gives the following recursive formula for the determinant of matrix M:

$$\begin{aligned}
M_0 &= -8\sqrt{3}\lambda_1^2 \\
M_m &= 12\lambda_{m+1}^2 \prod_{i=1}^{m} (\lambda_{m+1}^2 - \lambda_i^2)^3 \cdot M_{m-1},
\end{aligned}$$

where M_i represents the determinant of M for $m = i$. Recall that λ_j are non-repeated roots of $(-1)^m s$ with arguments in $(\pi/2, 3\pi/2)$. Therefore, $\lambda_i \neq 0$ and $\lambda_i \neq \pm\lambda_j$ for $i \neq j$. This guarantees that the determinant of M is not zero for any value of m and therefore the coefficients C_{ij} are unique. Thus all equal order problems are well-posed with at most algebraic growth in time if $\theta_i = 2\pi/3$.

The discussion above has assumed that $A_1 = A_2 = A_3$. We may also consider more general case with arbitrary A_i and consequently, different angle θ_i. However, no general determinant formula was found for these cases. Thus each case has to be considered separately. For example, when $m = 0$, the problem is described by system

$$\begin{aligned}
&\partial_t X_i \cdot N_i = A_i \kappa_i, \quad i = 1, 2, 3, \\
&\partial_\sigma X_i \cdot \partial_\sigma^2 X_i = 0, \quad i = 1, 2, 3.
\end{aligned} \tag{24}$$

The junction conditions are

$$\begin{aligned} &X_1(0,t) = X_2(0,t) = X_3(0,t),\\ &\partial_s X_1(0,t)\cdot\partial_s X_2(0,t) = \cos\theta_3,\\ &\partial_s X_1(0,t)\cdot\partial_s X_3(0,t) = \cos\theta_2, \end{aligned} \tag{25}$$

where θ_2, θ_3 now depend on A_i. A similar discussion can be applied to this curvature motion to obtain the determinant of the coefficient matrix M:

$$|M| = \frac{\omega\zeta\,\sin(\theta_2+\theta_3) - \lambda\zeta\,\sin\theta_3 - \lambda\omega\sin\theta_2}{\sin\theta_3\sin\theta_2\cos\theta_2\cos\theta_3}, \tag{26}$$

where λ, ω, ζ are given by

$$\lambda = -\sqrt{\frac{s}{A_1}}, \qquad \omega = -\sqrt{\frac{s}{A_2}}, \qquad \zeta = -\sqrt{\frac{s}{A_3}}, \tag{27}$$

with s temporarily being the Laplace transform variable.

We remark that, physically θ_i cannot be equal to or greater than π (this corresponds to zero or negative surface energy). Therefore, we only need to consider $0 < \theta_i < \pi$ and consequently we conclude that the determinant is not zero. For the case that one of the angles, for example $\theta_2 = \pi/2$, the determinant becomes undefined since $\cos\theta_2 = 0$. However, one may rotate the system such that Γ_2 points in the direction $(0,-1)^T$. Hence the above discussion still applies and the problem is well-posed if $0 < \theta_1, \theta_3 < \pi$. In summary, the problem of curvature motion is well-posed provided that $0 < \theta_i < \pi$ for $i = 1, 2, 3$.

A similar procedure can be applied to the fourth order surface diffusion problem discussed in Section 1 and the problem is well-posed provided $0 < \theta_i < \pi$.

The well-posedness of the above two cases has been discussed in [1,11], respectively with fully parabolic formulations. The approach in both studies is to linearize around the initial data and show the existence of the solution for the resulting linear system using the fundamental theory for parabolic system discussed in, e.g. [39]. The existence for the full nonlinear problem is then obtained by means of a fixed-point argument. The discussion in [1] has taken $A_i = 1$, though it is trivial to extend to arbitrary A_i. Note that artificial junction conditions are required in [11] for the surface diffusion problem. Our analysis gives the same result as in [1,11].

3. Mixed order problems

In this section, we consider some mixed order problems in which the phase boundaries may undergo different evolution laws. The system of equations has been proposed in the previous section as given in (14), i.e.

$$\begin{aligned} &\partial_t X_i \cdot N_i = (-1)^{m_i} A_i \partial_s^{2m_i}\kappa_i, \quad i = 1,2,3,\\ &\partial_\sigma X_i \cdot \partial_\sigma^2 X_i = 0, \quad i = 1,2,3, \end{aligned} \tag{28}$$

where $0 \le m_1 \le m_2 \le m_3$.

We again first assume $A_i = 1$ and impose the following junction conditions

$$\begin{aligned} &X_1(0,t) = X_2(0,t) = X_3(0,t),\\ &\partial_s X_1 \cdot \partial_s X_2 = \cos\theta_3,\\ &\partial_s X_1 \cdot \partial_s X_3 = \cos\theta_2,\\ &\partial_s^{2i-2}\kappa_1 + \partial_s^{2i-2}\kappa_2 + \partial_s^{2i-2}\kappa_3 = 0, \quad i = 1,\dots,m_1,\\ &\partial_s^{2i-1}\kappa_1 = \partial_s^{2i-1}\kappa_2 = \partial_s^{2i-1}\kappa_3, \quad i = 1,\dots,m_1,\\ &\partial_s^{2i-2}\kappa_2 + \partial_s^{2i-2}\kappa_3 = 0, \quad i = m_1+1,\dots,m_2,\\ &\partial_s^{2i-1}\kappa_2 = \partial_s^{2i-1}\kappa_3, \quad i = m_1+1,\dots,m_2,\\ &\partial_s^{2i-1}\kappa_3 = 0, \quad i = m_2+1,\dots,m_3. \end{aligned} \tag{29}$$

When $m_1 = 0$, $m_2 = m_3 = 1$, these conditions reduce to the junction conditions in (13) for the mixed order problem.

To discuss the well-posedness of the above system, the same approach as in Section 2.2 can be applied. However, no general determinant formula is found for this case. We can still verify case by case that all tested problems are well-posed. For example, if $m_1 = 1$, $m_2 = m_3 = 2$ and $\theta_i = 2\pi/3$, the determinant of the associated coefficients matrix M is given by

$$|M| \approx -2660.4\,i\left(1.4 + 2.0\,s^{1/12} + 5.7\,s^{2/12} + 12.0\,s^{3/12} + 2.8\,s^{4/12}\right)s^{39/12}.$$

Since both s and the roots of s have positive real part, one can easily verify that the determinant of M is not zero and the corresponding problem is well-posed with at most algebraic growth in time.

Similarly, when $m_1 = m_2 = 1$, $m_3 = 3$, the determinant of the resulting matrix is given by

$$|M| \approx (4369.6 + 18\,918.6\,s^{1/8} + 8739.3\,s^{2/8} + 2854.6\,s^{3/8} + 1809.9\,s^{4/8})s^{27/8}.$$

One can show that the determinant is not zero for any s satisfying the conditions (22) and (23) and therefore the corresponding problem is well-posed.

As the last example, we consider arbitrary A_i for $m_1 = 0$, $m_2 = 1$, $m_3 = 2$. The formulation for this problem is given by

$$\begin{aligned}
&\partial_t X_1 \cdot N_1 = A_1\kappa_1,\\
&\partial_t X_2 \cdot N_2 = -A_2\partial_s^2\kappa_2,\\
&\partial_t X_3 \cdot N_3 = A_3\partial_s^4\kappa_3,\\
&\partial_\sigma X_i \cdot \partial_\sigma^2 X_i = 0, \quad i = 1, 2, 3,
\end{aligned} \tag{30}$$

with the following conditions at the junction:

$$\begin{aligned}
&X_1(0, t) = X_2(0, t) = X_3(0, t),\\
&\partial_s X_1(0, t) \cdot \partial_s X_2(0, t) = \cos\theta_3,\\
&\partial_s X_1(0, t) \cdot \partial_s X_3(0, t) = \cos\theta_2,\\
&\gamma_2\kappa_2 + \gamma_3\kappa_3 = 0,\\
&A_2\partial_s^2\kappa_2 = A_3\partial_s^2\kappa_3,\\
&\partial_s^3\kappa_3 = 0.
\end{aligned} \tag{31}$$

Note that A_i and γ_i are present in these conditions.

One can again verify that the determinant for the associated coefficient matrix M is not zero and the problem is well-posed provided $0 < \theta_i < \pi$.

Similar results can be obtained for some other mixed order examples. They are all well-posed, with at most algebraic growth in time.

4. Numerical simulation

In this section, we consider numerical simulations for some of the high order problems including both the equal order case and the mixed order case. As the physical coefficients A_i impose no extra difficulty for numerical simulations, we take $A_i = 1$ for all examples in this section.

4.1. Simulation for equal order problems

For the equal order case, we consider an example that all curves are enclosed in a unit circle (see Fig. 3) and the normal velocity of each curve is equal to $\partial_s^4\kappa$. The system is described by

$$\begin{aligned}
&\partial_t X_i \cdot N_i = \partial_s^4\kappa_i, \quad i = 1, 2, 3,\\
&\partial_\sigma X_i \cdot \partial_\sigma^2 X_i = 0, \quad i = 1, 2, 3.
\end{aligned} \tag{32}$$

This is a sixth-order problem with $m = 2$ which requires twelve junction conditions as given below:

$$\begin{aligned}
&X_1(0, t) = X_2(0, t) = X_3(0, t),\\
&\partial_s X_1 \cdot \partial_s X_2 = \cos\theta_3,\\
&\partial_s X_1 \cdot \partial_s X_3 = \cos\theta_2,\\
&\kappa_1 + \kappa_2 + \kappa_3 = 0,\\
&\partial_s\kappa_1 = \partial_s\kappa_2 = \partial_s\kappa_3,\\
&\partial_s^2\kappa_1 + \partial_s^2\kappa_2 + \partial_s^2\kappa_3 = 0,\\
&\partial_s^3\kappa_1 = \partial_s^3\kappa_2 = \partial_s^3\kappa_3,
\end{aligned} \tag{33}$$

where $\theta_2 = \theta_3 = 2\pi/3$.

As this is a problem with a finite domain, we may specify a finite range for the parameter σ, e.g., [0, 1]. At the domain boundary where $\sigma = 1$, the following conditions are applied to each curve:

$$\begin{aligned}
&|X_i(1, t)| = 1,\\
&\partial_s X_i(1, t) \cdot T(X_i(1, t)) = 0,\\
&\partial_s^2\kappa_i = 0,\\
&\partial_s^3\kappa_i = 0.
\end{aligned} \tag{34}$$

The term $T(X(1))$ represents the tangential direction of the unit circle at point $X(1)$ and the first two conditions guarantee that the end of each curve is always attached perpendicularly to the circle.

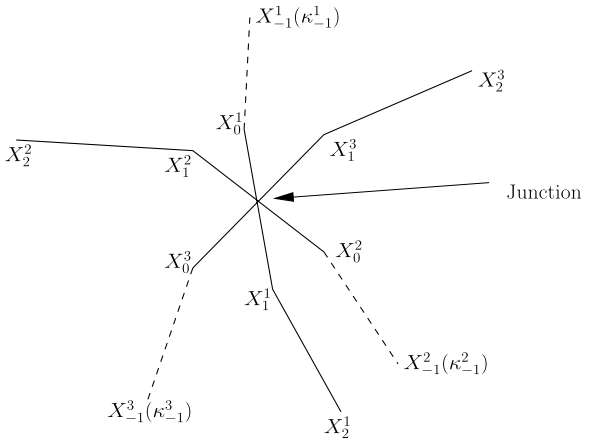

Fig. 2. Sketch of the ghost values at the triple junction for the discretization of the sixth order problem with $m = 2$. Two ghost points (X_0 and X_{-1}) and one ghost value (κ_{-1}) are introduced for each curve.

Before discussing the numerical discretization, we introduce an interesting property of this normal direction motion. Let V represent the normal velocity and c be the circumference of each phase. The normal velocity is either $V = \partial_s^4\kappa$ along the phase boundary or $V = 0$ along the domain boundary. Thus simple manipulation gives

$$\int_c V ds = 0, \tag{35}$$

by noticing the facts that $\partial_s^3\kappa_1 = \partial_s^3\kappa_2 = \partial_s^3\kappa_3$ at the junction and $\partial_s^3\kappa_i = 0$ at the domain boundary. This indicates that the area for each phase is preserved and this property can be also be used to test the performance of numerical methods.

The system can be discretized using standard finite difference schemes. The basic approach is to use a staggered grid in σ which is in the fixed interval [0,1] with $\sigma = 0$ at the junction and $\sigma = 1$ at the boundary of the computational domain. We shall denote the approximations by capital letters with subscripts, i.e., $X_j(t) \simeq X((j-1/2)h, t) = (u((j-1/2)h, t), v((j-1/2)h, t))$ where h is grid spacing and $N = 1/h$ is the number of interior grid points for $\sigma \in [0, 1]$. Here we use subscripts to represent the node index and we shall use superscripts to represent the curve index when necessary in the rest of this section.

We introduce some additional finite difference notations. Let D_k denote the second order centered approximation of the kth derivative, i.e.,

$$D_1X_j = (X_{j+1} - X_{j-1})/2h,$$
$$D_2X_j = (X_{j+1} + X_{j-1} - 2X_j)/h^2.$$

The curvature is then approximated by

$$\kappa_j = \frac{D_2X_j}{|D_1X_j|^2} \cdot (D_1X_j)^{\perp}. \tag{36}$$

Noticing the fact that σ is scaled arc length, the higher order derivatives of curvature can be approximated by

$$(\partial_s^2\kappa)_j = \frac{D_2\kappa_j}{|D_1X_j|^2}, \tag{37}$$

and

$$(\partial_s^4\kappa)_j = \frac{D_2(\partial_s^2\kappa)_j}{|D_1X_j|^2}. \tag{38}$$

The formulation maintains a strict equi-distributed grid which leads to a much simpler expression for the approximation of velocity $\partial_s^4\kappa$.

The discretization at the triple junction is subtle. When discretize using finite difference schemes with Neumann boundary conditions, a sixth order problem usually requires three ghost points and extra tangential conditions should be introduced at the junction. However, because of the lower order of the constraint equations in our formulation, it is possible to reduce the number of ghost points and avoid the use of artificial tangential conditions. For this sixth order problem, two ghost points X_0, X_{-1} and one ghost value κ_{-1} are introduced for each curve to approximate the conditions at the junction (see Fig. 2). The ghost value κ_{-1} denotes the curvature of the ghost point X_{-1} and it is used whenever the curvature of this

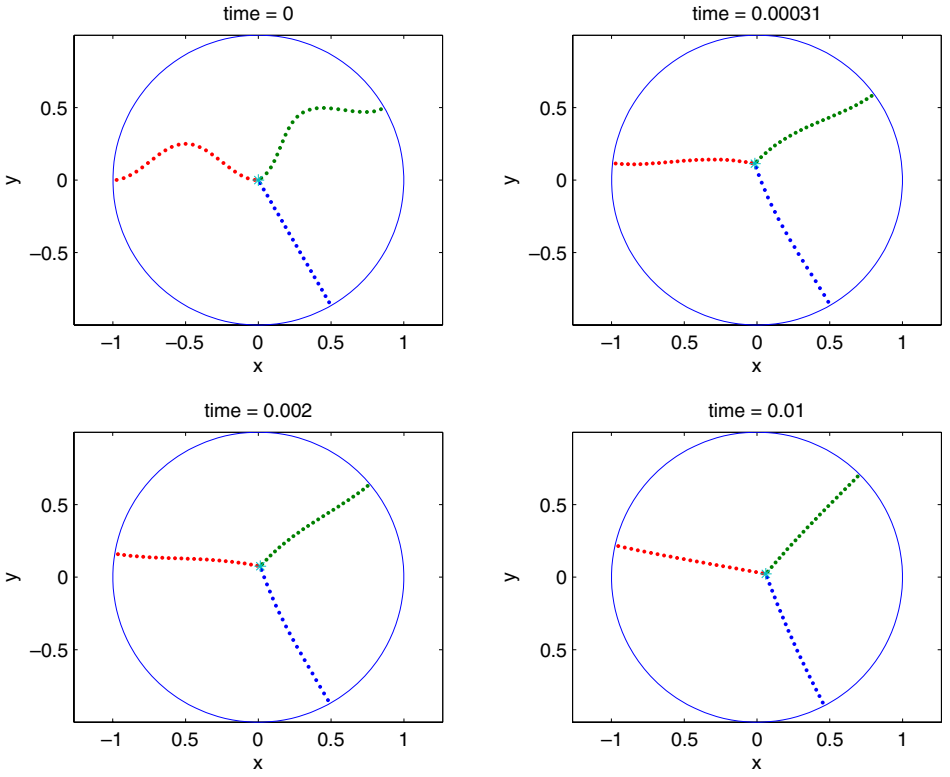

Fig. 3. Simulation of equal order problem with $m = 2$ (sixth order). Angles between curves at the triple junction are $2\pi/3$.

Table 1
Estimated errors and convergence rates for the equal order problem with $m = 2$ (sixth order). Errors are evaluated at $t = 1.2\text{e}{-4}$.

dt	h	$\|e_h\|_2$	ρ	$\|e_h\|_\infty$	ρ
$dt = 0.001h^2$	0.2	3.6804e−3		7.7141e−3	
	0.1	1.0309e−3	1.8360	2.0637e−3	1.9023
	0.05	2.9301e−4	1.8149	5.4136e−4	1.9306

point is required in an approximation. For more details, we refer to [7] where a similar discussion is available for a lower order problem.

To avoid the excessively small time steps due to the stiffness of the problem, we use implicit time-stepping. For simplicity we use the backward Euler method. It is found computationally that spatial errors dominate temporal errors. Since the three curves are strongly coupled by the junction, we solve for interior and ghost points simultaneously. The nonlinear system is solved by Newton's method.

The numerical results are shown in Fig. 3. As discussed before the area of each phase is preserved during the evolution. For example, the numerical result indicates that the area change for the top phase is less than 0.1%. To demonstrate the performance more quantitatively, we study the convergence rate of this method. Since the exact solution is not known we compare solution values to those at finer grids to estimate the error e_h:

$$e_h := \|\mathcal{X}_h - \mathcal{X}_{h/2}\| \tag{39}$$

where the subscript on $\mathcal{X}$ denotes the grid spacing used to compute the approximation and the norm $\|\cdot\|$ is the discrete norm. Note that interpolation must be used to compare the pointwise values of approximations at different grids. Successive error estimates can be used to estimate the convergence rate ρ as follows:

$$\rho \approx \rho_h := \log_2 \frac{e_{2h}}{e_h}. \tag{40}$$

Estimates of the error and convergence rate at $t = 1.2\text{e}{-4}$ are given in Table 1. The convergence rates are close to two.

4.2. Simulation for mixed order problems

The second numerical example is a mixed order problem with $m_1 = 0$, $m_2 = m_3 = 2$ which is described by

$$\begin{aligned} &\partial_t X_1 \cdot N_1 = \kappa_1, \\ &\partial_t X_i \cdot N_i = \partial_s^4 \kappa_i, \quad i = 2, 3, \\ &\partial_\sigma X_i \cdot \partial_\sigma^2 X_i = 0, \quad i = 1, 2, 3. \end{aligned} \tag{41}$$

For this problem, we propose a domain and initial settings as those in the coupled surface and grain boundary motion discussed in [7] (refer to Fig. 4).

This system requires ten junction conditions which are given by

$$\begin{aligned} &X_1(0, t) = X_2(0, t) = X_3(0, t), \\ &\partial_s X_1(0, t) \cdot \partial_s X_2(0, t) = \cos\theta_3, \\ &\partial_s X_1(0, t) \cdot \partial_s X_3(0, t) = \cos\theta_2, \\ &\kappa_2 + \kappa_3 = 0, \\ &\partial_s \kappa_2 = \partial_s \kappa_3, \\ &\partial_s^2 \kappa_2 + \partial_s^2 \kappa_3 = 0, \\ &\partial_s^3 \kappa_2 = \partial_s^3 \kappa_3, \end{aligned} \tag{42}$$

with values of θ_2, θ_3 prescribed.

It is known that the coupled surface and grain boundary motion, which is a lower mixed order problem, admits a traveling wave solution. The solution was given by Kanel et al. in [16] and we start our simulation with that solution. The reason we start with such a solution is that, the traveling wave solution to this higher order problem, if there is any, will stay close to that of the lower order problem so it can be converged to in a relatively short time. To maintain the curves flat at the far field domain boundary, we impose the following conditions:

$$\begin{aligned} &X_i(1, t) = \text{const}, \quad i = 1, 2, 3, \\ &\partial_s \kappa_i = 0, \quad i = 2, 3, \\ &\partial_s^2 \kappa_i = 0, \quad i = 2, 3, \\ &\partial_s^3 \kappa_i = 0, \quad i = 2, 3 \end{aligned} \tag{43}$$

where the const depends on the domain size.

The discretization of the junction and boundary conditions again requires some ghost points and ghost values which can be introduced analogously. The numerical results are shown in Fig. 4. The simulation shows that the shape of the curves stabilizes after a while and then moves to the right at a constant speed. The speed of the triple junction versus time is drawn in Fig. 5 and it clearly converges to a constant speed. This result indicates the possible existence of traveling wave solutions.

We remark that all curvature dependent motions discussed in this paper that are fourth-order or higher are area preserving. Therefore, no traveling wave solution is possible if $m_i \geq 1$ for all three curves. The following problem is an example that does not have traveling wave solution.

We consider a mixed order problem with $m_1 = 1$, $m_2 = m_3 = 2$. This problem is described by the following system:

$$\begin{aligned} &\partial_t X_1 \cdot N_1 = -\partial_s^2 \kappa_1, \\ &\partial_t X_i \cdot N_i = \partial_s^4 \kappa_i, \quad i = 2, 3, \\ &\partial_\sigma X_i \cdot \partial_\sigma^2 X_i = 0, \quad i = 1, 2, 3. \end{aligned} \tag{44}$$

The corresponding junction conditions are given by

$$\begin{aligned} &X_1(0, t) = X_2(0, t) = X_3(0, t), \\ &\partial_s X_1(0, t) \cdot \partial_s X_2(0, t) = \cos\theta_3, \\ &\partial_s X_1(0, t) \cdot \partial_s X_3(0, t) = \cos\theta_2, \\ &\kappa_1 + \kappa_2 + \kappa_3 = 0, \\ &\partial_s \kappa_1 = \partial_s \kappa_2 = \partial_s \kappa_3, \\ &\partial_s^2 \kappa_2 + \partial_s^2 \kappa_3 = 0, \\ &\partial_s^3 \kappa_2 = \partial_s^3 \kappa_3, \end{aligned} \tag{45}$$

with values of θ_2, θ_3 prescribed.

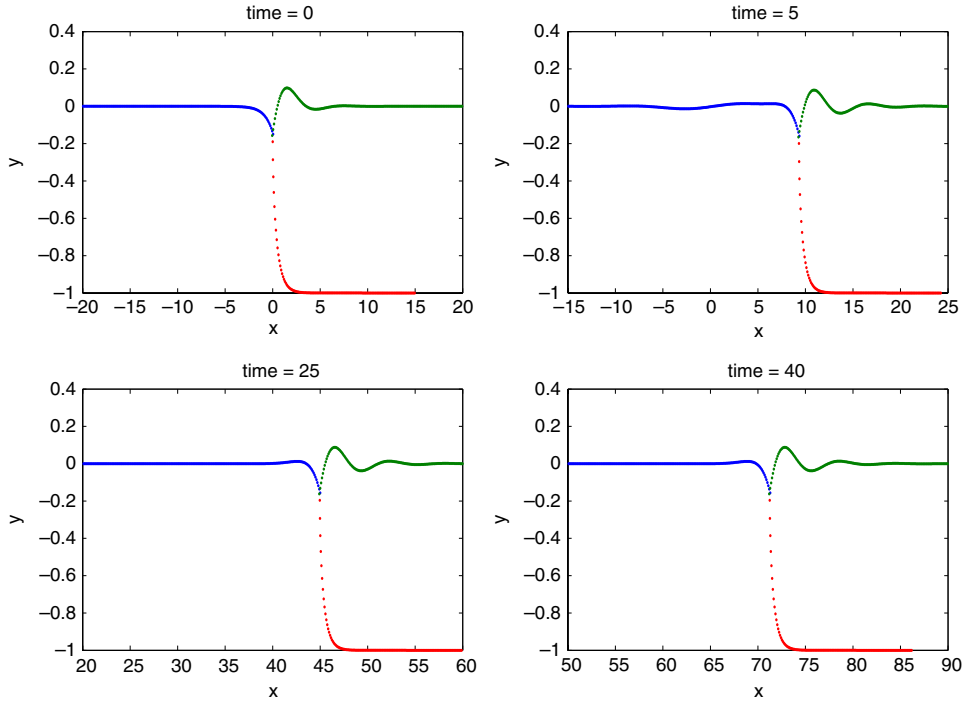

Fig. 4. Simulation of mixed order problem with $m_1 = 0$, $m_2 = m_3 = 2$.

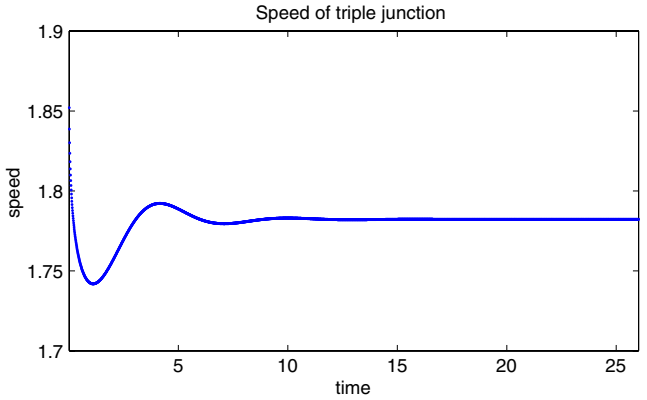

Fig. 5. Plot of the junction speed versus time for the mixed order problem with $m_1 = 0$, $m_2 = m_3 = 2$.

We again start the simulation with the traveling wave solution for the coupled surface and grain boundary motion. The following conditions are imposed at the domain boundary:

$$\begin{aligned} &X_i(1, t) = \text{const}, \quad i = 1, 2, 3, \\ &\partial_s \kappa_i = 0, \quad i = 1, 2, 3, \\ &\partial_s^2 \kappa_i = 0, \quad i = 2, 3, \\ &\partial_s^3 \kappa_i = 0, \quad i = 2, 3. \end{aligned} \tag{46}$$

The discretization of this system is similar to previous examples. The numerical results are shown in Fig. 6. We do not expect any traveling wave solutions for this problem due to the reason stated before. A perturbation appears on the bottom phase boundary during the evolution and it seems to grow unboundedly.

5. Conclusions

In this paper, we discuss a class of high order three-phase boundary motion problems. Formulations that automatically maintain an uniform grid spacing when discretized are proposed to describe the problems in this class. All problems are

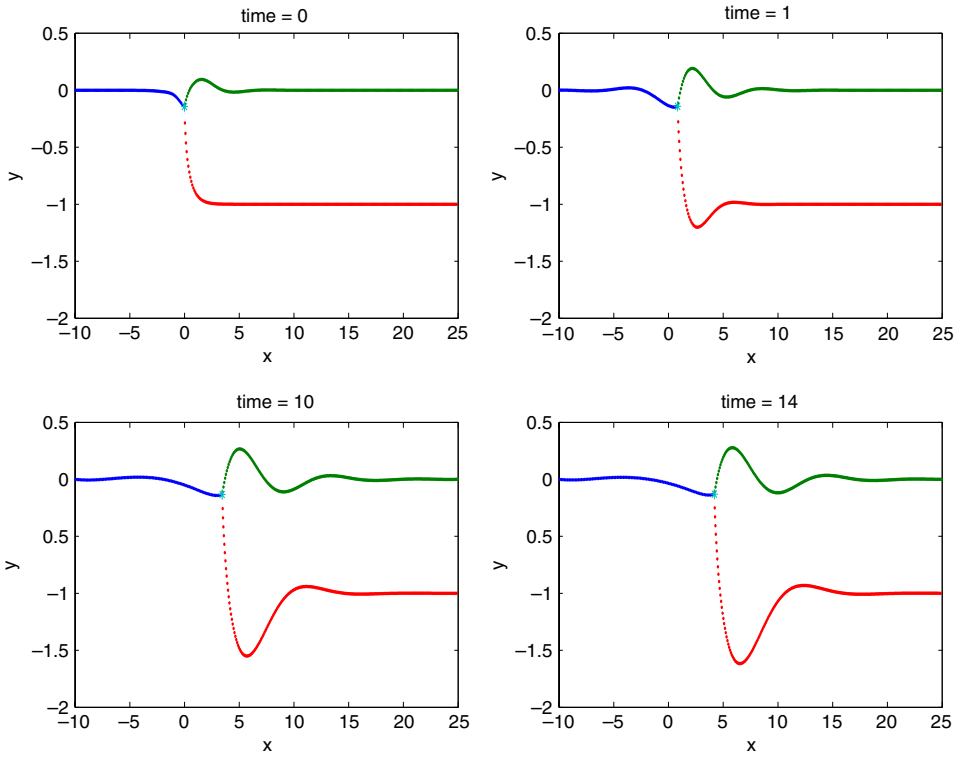

Fig. 6. Simulation of mixed order problem with $m_1 = 1$, $m_2 = m_3 = 2$.

shown to be well-posed when all three curves evolve under the same evolution law. When two or more types of motion are involved, we investigate the well-posedness case by case. All cases that we considered are well-posed.

Numerical simulations are performed for some examples including both equal order problems and mixed order problems using finite difference schemes on a staggered grid. Convergence rate of the numerical method is also studied by estimating errors with approximations over different grids and the convergence rate is close to two. The numerical results also suggest the possible existence of traveling wave solutions for some mixed order problems. In future work, we could investigate these waves analytically if possible.

References

[1] L. Bronsard, F. Reitich, On three-phase boundary motion and the singular limit of a vector-valued Ginzburg–Landau equation, Archive for Rational Mechanics and Analysis 124 (4) (1993) 355–379.
[2] L. Bronsard, B.T.R. Wetton, A numerical method for tracking curve networks moving with curvature motion, Journal of Computational Physics 120 (1) (1995) 66–87.
[3] U. Czubayko, V.G. Sursaeva, G. Gottstein, L.S. Shvindlerman, Influence of triple junctions on grain boundary motion, Acta Materialia 46 (16) (1998) 5863–5871.
[4] B. Merriman, J.K. Bence, S.J. Osher, Motion of multiple junctions: a level set approach, Journal of Computational Physics 112 (2) (1994) 334–363.
[5] W. Mullins, Two-dimensional motion of idealized grain boundaries, Journal of Applied Physics 27 (1956) 900–904.
[6] S. Osher, J.A. Sethian, Fronts propagating with curvature-dependent speed: algorithms based on Hamilton–Jacobi formulations, Journal of Computational Physics 79 (1) (1988) 12–49.
[7] Z. Pan, B.T. Wetton, A numerical method for coupled surface and grain boundary motion, European Journal of Applied Mathematics 19 (2008) 311–327.
[8] G. Gottstein, L. Shvindlerman, Grain Boundary Migration in Metals: Thermodynamics, Kinetics, Applications, CRC Press, 1999.
[9] J.W. Barrett, H. Garcke, R. Nürnberg, On the variational approximation of combined second and fourth order geometric evolution equations, SIAM Journal on Scientific Computing 29 (3) (2007) 1006–1041.
[10] D.L. Chopp, J. Sethian, Motion by intrinsic Laplacian of curvature, Interfaces and Free Boundaries 1 (1999) 1–18.
[11] H. Garcke, A. Novick-Cohen, A singular limit for a system of degenerate Cahn–Hilliard equations, Advanced Differential Equations 5 (2000) 401–434.
[12] Z. Pan, B. Wetton, Numerical methods for coupled surface and grain boundary motion. arXiv report math.NA/0702503. Available at: http://arxiv.org/.
[13] W. Mullins, Theory of thermal grooving, Journal of Applied Physics 28 (1957) 333–339.
[14] C. Dunn, F. Daniels, M. Bolton, Transactions of the American Institute of Mining, Metallurgical and Petroleum Engineers 185 (1949) 708.
[15] J. Kanel, A. Novick-Cohen, A. Vilenkin, A traveling wave solution for coupled surface and grain boundary motion, Acta Materialia 51 (7) (2003) 1981–1989.
[16] J. Kanel, A. Novick-Cohen, A. Vilenkin, Coupled surface and grain boundary motion: A travelling wave solution, Nonlinear Analysis 59 (8) (2004) 1267–1292.
[17] J. Kanel, A. Novick-Cohen, A. Vilenkin, Coupled surface and grain boundary motion: Nonclassical traveling wave solution, Advanced Differential Equations 9 (2004) 299–327.
[18] J. Kanel, A. Novick-Cohen, A. Vilenkin, A numerical study of grain boundary motion in bicrystals, Acta Materialia 53 (2) (2005) 227–235.
[19] D. Min, H. Wong, A model of migrating grain-boundary grooves with application to two mobility-measurement methods, Acta Materialia 50 (20) (2002) 5155–5169.

[20] W. Mullins, The effect of thermal grooving on grain boundary motion, Acta Materialia 6 (1958) 414–427.
[21] A.J. Vilenkin, R. Kris, A. Brokman, Breakup and grain growth in thin-film array, Journal of Applied Physics 81 (1) (1997) 238–245.
[22] H. Zhang, H. Wong, Coupled grooving and migration of inclined grain boundaries: regime I, Acta Materialia 50 (8) (2002) 1983–1994.
[23] H. Zhang, H. Wong, Coupled grooving and migration of inclined grain boundaries: regime II, Acta Materialia 50 (8) (2002) 1995–2012.
[24] W. Zhang, J.H. Schneibel, Numerical simulation of grain-boundary grooving by surface diffusion, Computational Materials Science 3 (3) (1995) 347–358.
[25] J. Sethian, Level Set Methods and Fast Marching Methods: Evolving Interfaces in Computational Geometry, Fluid Mechanics, Computer Vision, and Materials Science, in: Cambridge Monographs on Applied and Computational Mathematics, vol. 3, Cambridge University Press, 1999.
[26] S. Osher, R. Fedkiw, Level Set Methods and Dynamic Implicit Surfaces, in: Applied Mathematical Sciences, vol. 153, Springer, 2003.
[27] K.A. Smith, F.J. Souls, D.L. Chopp, A projection method for motion of triple junctions by level sets, Interfaces and Free Boundaries 4 (2002) 263–276.
[28] H.-K. Zhao, T. Chan, B. Merriman, S. Osher, A variational level set approach to multiphase motion, Journal of Computational Physics 127 (1) (1996) 179–195.
[29] B. Merriman, J.K. Bence, S.J. Osher, Diffusion generated motion by mean curvature, in: J. Taylor (Ed.), Computational Crystal Growers Workshop, American Mathematical Society, Providence, Rhode Island, 1992, pp. 73–83.
[30] S. Esedoglu, S. Ruuth, R. Tsai, Threshold dynamics for high order geometric motions, Interfaces and Free Boundaries 10 (3) (2008) 263–282.
[31] B. Merriman, S.J. Ruuth, Diffusion generated motion of curves on surfaces, Journal of Computational Physics 225 (2) (2007) 2267–2282.
[32] S.J. Ruuth, Efficient algorithms for diffusion-generated motion by mean curvature, Journal of Computational Physics 144 (2) (1998) 603–625.
[33] J. Cahn, A. Novick-Cohen, Evolution equations for phase separation and ordering in binary alloys, Journal of Statistical Physics 76 (3) (1994) 877–909.
[34] J.W. Cahn, A. Novick-Cohen, Motion by curvature and impurity drag: resolution of a mobility paradox, Acta Materialia 48 (13) (2000) 3425–3440.
[35] A. Novick-Cohen, Triple-junction motion for an Allen–Cahn/Cahn–Hilliard system, Physica D. Nonlinear Phenomena 137 (1–2) (2000) 1–24.
[36] J.W. Barrett, J.F. Blowey, H. Garcke, On fully practical finite element approximations of degenerate Cahn–Hilliard systems, M2AN. Mathematical Modelling and Numerical Aanalysis 35 (4) (2001) 713–748.
[37] H.G. Lee, J. Kim, A second-order accurate non-linear difference scheme for the *n*-component Cahn–Hilliard system, Physica A: Statistical Mechanics and its Applications 387 (19–20) (2008) 4787–4799.
[38] J.W. Barrett, H. Garcke, R. Nürnberg, A phase field model for the electromigration of intergranular voids, Interfaces and Free Boundaries 9 (2007) 171–210.
[39] V. Solonnikov, Boundary value problems in physics, Proceedings of the Steklov Institute of Mathematics LXXXIII (1965).